QCD CRITICAL POINT IN THE STRONG COUPLING LATTICE QCD AND DURING BLACK HOLE FORMATION*

A. Ohnishi[a], K. Miura[b], T.Z. Nakano[a,c], N. Kawamoto[d]
H. Ueda[c], M. Ruggieri[a,e], K. Sumiyoshi[f]

[a]Yukawa Institute for Theoretical Physics, Kyoto University
Kyoto 606-8502, Japan
[b]INFN Laboratori Nazionali di Frascati, 00044 Frascati (RM), Italy
[c]Department of Physics, Faculty of Science, Kyoto University
Kyoto 606-8502, Japan
[d]Department of Physics, Faculty of Science, Hokkaido University
Sapporo 060-0810, Japan
[e]Department of Physics and Astronomy, University of Catania
Via S. Sofia 64, 95125 Catania, Italy
[f]Numazu College of Technology, Ooka 3600, Numazu, Shizuoka 410-8501, Japan

We discuss the QCD phase diagram from two different points of view. We first investigate the phase diagram structure in the strong coupling lattice QCD with Polyakov loop effects, and show that the chiral and Z_{N_c} deconfinement transition boundaries deviate at finite μ as suggested from large N_c arguments. Next, we discuss the possibility to probe the QCD critical point during prompt black hole formation processes. The thermodynamical evolution during the black hole formation would result in quark matter formation, and the critical point in isospin asymmetric matter may be swept. (T, μ_B) region probed in heavy-ion collisions and the black hole formation processes cover most of the critical point locations predicted in recent lattice Monte Carlo simulations and chiral effective models.

1. Introduction

QCD phase transition at finite temperature (T) and chemical potential (μ) has been attracting much attention in recent years. The beam energy and system size scan programs at RHIC [1] and SPS [2] are running to discover

---

the critical point and the first order transition at finite T and μ, and the discovery of the two solar mass neutron star [3] gives us some hints on the phase transition at finite density. Recent large N_c arguments suggest the existence of another form of matter, referred to as the quarkyonic matter, where the Polyakov loop is suppressed and the density is high [4].

In this proceedings, we first discuss the chiral and Z_{N_c} deconfinement transitions at finite T and μ based on the strong coupling lattice QCD with Polyakov loop effects (P-SC-LQCD) [5]. Next, we discuss the possibility to probe the critical point in isospin asymmetric high baryon density matter formed during the prompt black hole formation processes [6].

2. Strong coupling lattice QCD and quarkyonic matter

Do the chiral and Z_{N_c} deconfinement transition boundaries deviate at large μ? This is one of the most interesting questions in the current QCD phase diagram studies. From the large N_c arguments, we expect the existence of the so-called quarkyonic matter, where the Z_{N_c} order parameter (Polyakov loop) is suppressed and the density is high [4]. In the lattice QCD Monte Carlo simulations at $\mu = 0$, the Z_{N_c} transition temperature $(T_c(Z_{N_c}))$ is close to but somewhat larger than the chiral transition temperature $(T_c(\chi))$ [7]. In chiral effective models, some of them predict the existence of quarkyonic-like matter [8, 9], while some of them predict that the Z_{N_c} transition boundary agrees with the chiral transition boundary [10]. Thus it is important to discuss the chiral and Z_{N_c} transition boundaries at finite μ in the theoretical framework directly based on QCD for $N_c = 3$.

The strong coupling $(1/g^2)$ expansion in the lattice QCD (SC-LQCD) has been successful since the beginning of the lattice gauge theory [11] and would provide an alternative lattice framework to study the QCD phase diagram at finite T and μ [12, 13]. For example, the spontaneous breaking of the chiral symmetry and its restoration at finite T and/or μ have been known to be realized in the strong coupling limit [13]. Recently, the finite couping and Polyakov loop effects are incorporated in the framework of SC-LQCD, and are found to explain the MC results of T_c at $\mu = 0$ in the region $\beta = 2N_c/g^2 \lesssim 4$ [5, 14], as shown in the left panel of Fig. 1.

We discuss here the chiral and Z_{N_c} deconfinement dynamics by using the SC-LQCD with the Polyakov loop effects (P-SC-LQCD) in the mean field approximation [5]. We take account of the next-to-leading order (NLO, $\mathcal{O}(1/g^2)$) and the leading order $(\mathcal{O}(1/g^{2N_\tau}))$ of the strong coupling expansion in the fermionic and pure gluonic sector, respectively, and in the leading order of the $1/d$ expansion [15]. The effective potential is given as [5]

$$\mathcal{F}_{\text{eff}}(\Phi; T, \mu) \equiv -(T \log \mathcal{Z}_{\text{LQCD}})/N_s^d = \mathcal{F}_{\text{eff}}^\chi + \mathcal{F}_{\text{eff}}^{\text{Pol}}, \tag{1}$$

$$\mathcal{F}_{\text{eff}}^{\chi} \simeq \left(\frac{d}{4N_c} + \beta_s\varphi_s\right)\sigma^2 + \frac{\beta_s\varphi_s^2}{2} + \frac{\beta_\tau}{2}\left(\varphi_\tau^2 - \omega_\tau^2\right) - N_c\log\sqrt{Z_+Z_-}$$
$$- N_cE_q - T\left[\log\mathcal{R}\left(E_q - \tilde{\mu}, \ell, \bar{\ell}\right) + \log\mathcal{R}\left(E_q + \tilde{\mu}, \ell, \bar{\ell}\right)\right] , \quad (2)$$

$$\mathcal{F}_{\text{eff}}^{\text{Pol}} \simeq -2TdN_c^2\left(\frac{1}{g^2N_c}\right)^{1/T}\bar{\ell}\ell - T\log\mathcal{M}_{\text{Haar}}\left(\ell, \bar{\ell}\right) , \quad (3)$$

$$\tilde{\mu} = \mu - \log\sqrt{Z_+/Z_-} , \qquad Z_{\pm} = 1 + \beta_\tau(\varphi_\tau \pm \omega_\tau) ,$$
$$\mathcal{R}\left(x, \ell, \bar{\ell}\right) \equiv 1 + N_c\ell e^{-x/T} + N_c\bar{\ell}e^{-2x/T} + e^{-3x/T} , \quad (4)$$
$$\mathcal{M}_{\text{Haar}}\left(\ell, \bar{\ell}\right) = 1 - 6\bar{\ell}\ell - 3\left(\bar{\ell}\ell\right)^2 + 4\left(\ell^3 + \bar{\ell}^3\right) , \quad (5)$$

where σ and $\ell(\bar{\ell})$ denote the chiral condensate and the (anti-)Polyakov loop, respectively, $d = 3$ is the spatial dimension, $\beta_\tau = \beta d/2N_c^3$ and $\beta_s = \beta d(d - 1)/16N_c^5$. E_q is the quark excitation energy which is a function of σ and other auxiliary fields. Several other auxiliary fields $(\varphi_s, \varphi_\tau, \omega_\tau)$ are introduced in addition to σ and ℓ, and the stationary conditions are imposed on these fields in equilibrium. The Polyakov loop ℓ couples with quarks, and appears with the Boltzmann factor $e^{-(E_q - \tilde{\mu})/T}$. Color-singlet states dominate in the confined phase ($\ell \sim 0$), while quarks can excite in the deconfined phase ($\ell \neq 0$). This issue has been pointed out in the strong coupling limit and utilized in the PNJL model [16].

We discuss the results at $\beta = 4$, which is in the coupling range, where P-SC-LQCD roughly explains the LQCD-MC results of T_c at $\mu = 0$, and results are shown in the lattice unit, $a = 1$. In the right panel of Fig. 1,
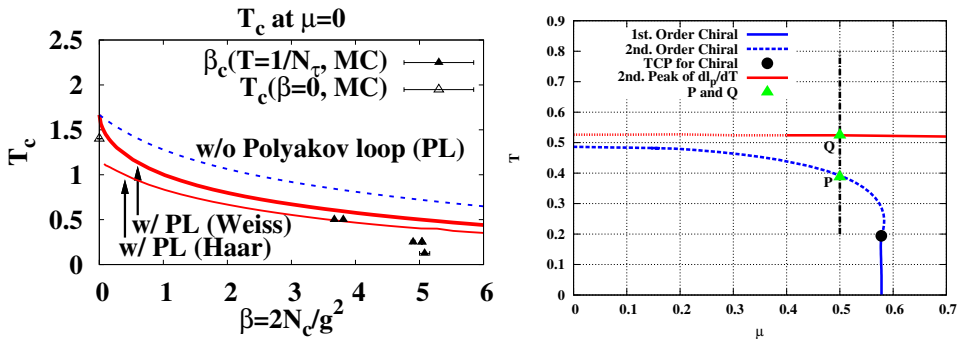

Fig. 1. Left: Comparison of T_c at $\mu = 0$ in P-SC-LQCD (solid) and SC-LQCD (without the Polyakov loop, dashed) [5]. Two different Polyakov loop treatments (Weiss and Haar method) are compared. The triangles represent the lattice MC results with one species of unrooted staggered fermion. Right: The phase boundary for the chiral transition with the second peak of $d\ell/dT$ at $\beta = 4$ in the chiral limit. The "P" and "Q" correspond to those in Fig. 2.

we show the phase diagram at $\beta = 4$ in the chiral limit ($m_0 = 0$). We find the second-(dashed) and first-order (solid) chiral transition boundaries separated by the (tri-)critical point (CP) at $(\mu_{\mathrm{CP}}, T_{\mathrm{CP}}) = (0.58, 0.19)$.

In the left panel of Fig. 2, we show the T dependence of the chiral condensate σ and the Polyakov loop ℓ at $\mu = 0.5$. At the chiral transition temperature, the chiral condensate becomes zero quickly, and the Polyakov loop is affected to have a kink. In addition to this chiral-induced kink shown as "P" in the figure, we find another temperature shown as "Q", where the Polyakov loop increases rapidly. This feature is more clearly seen in $d\ell/dT$. We show $d\ell/dT$ at $\mu = 0.5$ and $m_0 = 0.03$ in the right panel of Fig. 2. We can see the second peak in $d\ell/dT$ at $T_Q \sim 0.52$. A similar double-peak structure has been reported in the model studies based on PNJL model [9].
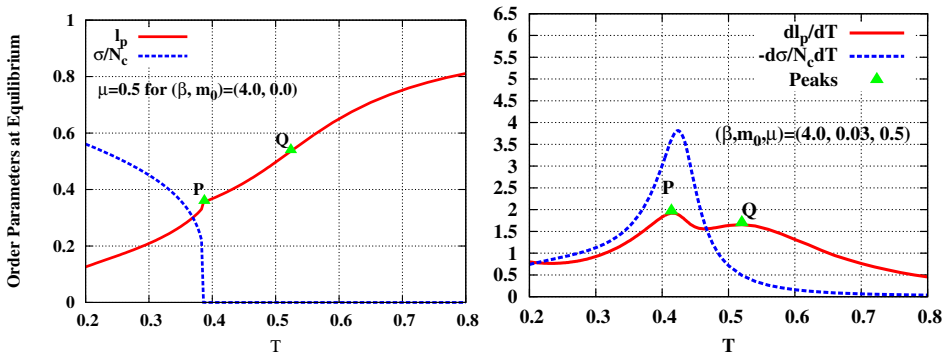

Fig. 2. Left: T dependence of the chiral condensate (dashed) and the Polyakov loop (solid) at $\mu = 0.5$ and $\beta = 4$ in the chiral limit. "P" and "Q" correspond to the points in the right panel of Fig. 1. Right: T dependence of $d\sigma/dT$ (dashed) and $d\ell/dT$ (solid) with $m_0 = 0.03$ at $\beta = 4$ and $\mu = 0.5$.

The peak "Q" can be understood as the Z_{N_c}-induced crossover for the following reasons. The temperature $T_Q \sim 0.52$ is found to be almost independent on the chemical potential, as indicated by the upper line in the right panel of Fig. 1. T_Q is also insensitive to quark mass. The temperature of the peak "P" is shifted upward and becomes closer to "Q" with increasing m_0, while T_Q stays almost constant. For larger masses, $m_0 > 0.05$, the two peaks merge to a single peak, and the height of this single peak grows with increasing m_0 at temperature which is nearly m_0 independent. These observations agree with the expected character of the Z_{N_c}-induced transition; the Z_{N_c} deconfinement transition nature would be stronger with large quark mass, and its transition temperature would show a small dependence on μ from the large N_c argument. This interpretation supports the existence of the quarkyonic-like phase in cold-dense matter, characterized by high density and small Polyakov loop expectation value.

3. Critical point sweep during black hole formation

Critical point (CP) is one of the largest targets in the beam energy and system size scan programs at RHIC and SPS and in the forthcoming FAIR facility. CP is expected to be probed in these experiments if it is in the low baryon chemical potential region, $\mu_{\mathrm{CP}} \lesssim 500$ MeV, as predicted in some of the lattice MC calculations [26, 27, 28]. On the other hand, we cannot reject the possibility that the CP is located in the lower T and higher μ region, as predicted in many of the chiral effective models [21, 16, 22, 23, 24]. Therefore, it is important to search for other candidate sites, where hot and dense matter is formed and CP is reachable.

A gravitational collapse of a massive star is a promising candidate. A majority of non-rotating massive stars with mass $M \gtrsim 20M_{\odot}$ are expected to collapse quietly (faint-supernova) to black holes (BH) [18]. Their frequency should be comparable to supernovae, provided that the mass spectrum of stars has a long tail as in the power law behavior. The BH formation processes are found to form hot ($T \sim 90$ MeV) and dense ($\rho_B \sim 4\rho_0$) matter in the neutrino-radiation hydrodynamical simulations in the collapse and bounce stage of a $40M_{\odot}$ star [19]. Thermodynamical variables at a given time vary as a function of radius in a proto-neutron star and form a line (referred to as the BH formation profile in the later discussions) in the $T-\mu_B$ plane. In Fig. 3, we show the BH formation profile $(T, \mu_B, \delta\mu)$ [19] calculated by using the Shen EOS at $t = 0.5, 1.0$ and 1.344 sec after the bounce during the BH formation from a 40 $M_{\odot}$ star in the proto-neutron star core, where the mass coordinate from the center is $M < 1.6M_{\odot}$. The time $t = 1.344$ sec is just before the horizon formation. From the outer to the inner region of the proto-neutron star, T first increases from $T \sim 10$ MeV to $T \sim$ (50–90) MeV in the middle heated region, and decreases again inside. The baryon chemical potential μ_B is found to go over 1300 MeV in the central region just before the horizon formation at $t = 1.344$ sec. The isospin chemical potential is found to be $\delta\mu = $ (50–130) MeV in the inner region. The temperature and density in BH formation are significantly higher than in the model explosion calculation of supernova. The highest temperature and density are moderate in the collapse and bounce stage of supernovae, $(T, \rho_B) \sim (21.5$ MeV, 0.24 fm$^{-3})$ when hadronic EOS is adopted [20], while it has been argued that the transition to quark matter might trigger a successful supernovae [17].

We discuss here the possibility that the BH formation profile evolves with time and may pass through CP and the vicinity (*CP sweep*). The CP location scatters in the $T-\mu_B$ plane in chiral effective models such as NJL [21], P-NJL [16, 22], P-NJL with 8-quark interaction (P-NJL$_8$) [23], and PQM [24] models. We expect that CP moves in the lower T direction
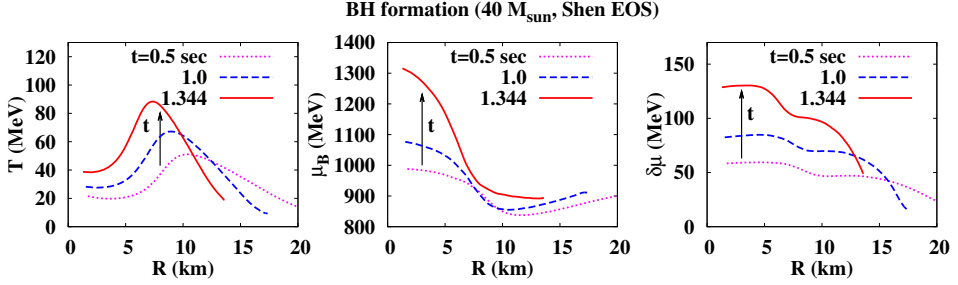
BH formation (40 M$_{sun}$, Shen EOS)

Fig. 3. The BH formation profile, $(T, \mu_B, \delta\mu)$, as a function of the radius. Results are shown for the gravitational collapse of a 40 $M_\odot$ star at $t = 0.5$ sec (dotted), 1.0 sec (dashed), and 1.344 sec (solid lines, just before the horizon formation).

at finite $\delta\mu$, because d-quark dominates and the effective number of flavors decreases. Since the matter passes through the high μ_B and low T region compared with high-energy heavy-ion collisions, the reduction of the CP temperature T_{CP} is essential for the CP sweep during the BH formation.

The Lagrangian density of the Polyakov loop extended quark meson (PQM) model, as an example of chiral effective models, is given by

$$
\begin{aligned}
\mathcal{L} &= \bar{q}\left[i\gamma^\mu D_\mu - g\left(\sigma + i\gamma_5 \boldsymbol{\tau}\cdot\boldsymbol{\pi}\right) - g_v\gamma^\mu\left(\omega_\mu + \boldsymbol{\tau}\cdot\boldsymbol{R}_\mu\right)\right]q \\
&+ \tfrac{1}{2}(\partial_\mu\sigma)^2 + \tfrac{1}{2}(\partial_\mu\boldsymbol{\pi})^2 - U(\sigma, \boldsymbol{\pi}) - \mathcal{U}_\ell(\ell, \bar{\ell}, T) \\
&- \tfrac{1}{4}\omega_{\mu\nu}\omega^{\mu\nu} - \tfrac{1}{4}\boldsymbol{R}_{\mu\nu}\cdot\boldsymbol{R}^{\mu\nu} + \tfrac{1}{2}m_v^2(\omega_\mu\omega^\mu + \boldsymbol{R}_\mu\cdot\boldsymbol{R}^\mu)\,.
\end{aligned} \tag{6}
$$

The mesonic potential is $U(\sigma, \boldsymbol{\pi}) = \lambda\left(\sigma^2 + \boldsymbol{\pi}^2 - v^2\right)^2/4 - h\sigma$, and $\omega_{\mu\nu}$ and $\boldsymbol{R}_{\mu\nu}$ are the field tensors of the ω and ρ mesons. We use the Polyakov loop effective potential $\mathcal{U}_\ell(\ell, \bar{\ell}, T) = T^4[-a(T)\bar{\ell}\ell/2 + b(T)\log H(\ell, \bar{\ell})]$, where the Polyakov loop is defined as $\ell = \text{Tr}[\mathcal{P}\exp(i\int_0^{1/T} d\tau A_4)]/N_c$. In the mean field approximation, the thermodynamic potential is obtained as

$$
\begin{aligned}
\Omega_{PQM} &= U_\sigma + \mathcal{U}_\ell - \frac{g_v^2}{m_v^2}\left(\rho_u^2 + \rho_d^2\right) - 2N_f N_c \int^\Lambda \frac{d^3\boldsymbol{p}}{(2\pi)^3} E_p \\
&- 2T\sum_f \int \frac{d^3\boldsymbol{p}}{(2\pi)^3}\left[\log\mathcal{R}\left(E_p - \tilde{\mu}, \ell, \bar{\ell}\right) + \log\mathcal{R}\left(E_p + \tilde{\mu}, \bar{\ell}, \ell\right)\right]\,, \tag{7}
\end{aligned}
$$

where $E_p = \sqrt{\boldsymbol{p}^2 + M^2}$, $M = g\sigma + m_0$ is the constituent quark mass, and $\tilde{\mu}_f = \mu \mp \delta\mu - 2g_v^2\rho_f/m_v^2$ is the effective chemical potential with $\mp = -, +$ for $f = u$ and d, respectively. While the PQM model is renormalizable, we adopt here the momentum cutoff Λ for simplicity.

We show the first order phase boundary of symmetric ($\delta\mu = 0$) and asymmetric ($\delta\mu \neq 0$) matter in PQM in the left panel of Fig. 4. We find a trend that the first order phase boundary shrinks at finite $\delta\mu$. Transition temperature at a given baryon chemical potential $\mu_B = 3\mu$ decreases, and the transition baryon chemical potential μ_c at $T = 0$ also decreases. We do not consider here the pion condensed phase, because the s-wave πN repulsion would suppress the s-wave pion condensation [25].
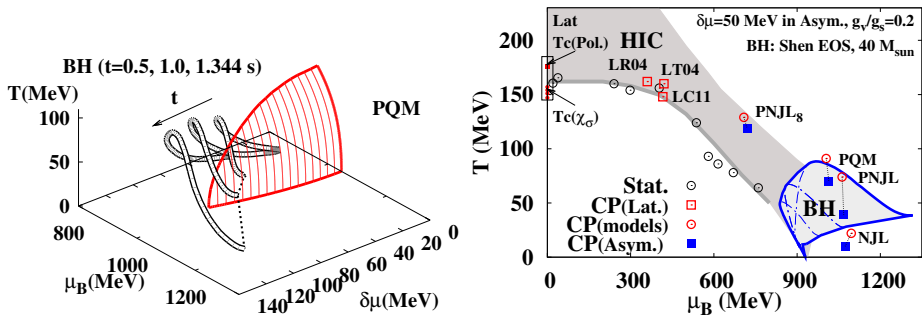

Fig. 4. Left: First order phase boundary surface (solid lines) in $(T, \mu_B, \delta\mu)$ space calculated with the PQM model are compared with the BH formation profile, (thermodynamical profile $(T, \mu_B, \delta\mu)$ during the BH formation) at $t = 0.5, 1.0, 1.344$ sec after the bounce (double lines). Right: Predictions of the critical temperature and critical point locations in comparison with the chemical freeze-out points and the swept region during the black hole formation.

The CP location is sensitive to $\delta\mu$. Compared with the results in symmetric matter, T_{CP} becomes smaller at finite $\delta\mu$ and reaches zero at $\delta\mu = \delta\mu_c \simeq (50-80)$ MeV. CP is also sensitive to the model and parameters as shown in the right panel of Fig. 4. The Polyakov loop suppresses single quark excitations in the hadron phase, then the transition temperature and thus the critical temperature are shifted upwards in the P-NJL model. The temporal component of the vector potential shifts the chemical potential effectively, and consequently leads to an upward shift of μ_c by about 10–15 MeV at $g_v/g = 0.2$.

We shall now compare the CP location and the phase boundary with the BH formation profile. In the left panel of Fig. 4, we compare the phase boundaries and the BH formation profile in the PQM model. During the BH formation, the baryon chemical potential reaches around 1000, 1100 and 1300 MeV in the central region of the proto-neutron star at $t = 0.5, 1.0$ and 1.344 sec, respectively, suggesting that quark matter would be formed between $t = 0.5$ and 1.0 sec in the central region in most of the models considered here. We also find that the BH profile goes through the critical line in asymmetric matter, *i.e.* the CP sweep takes place in PQM. In other

models, we find that there are three possible types in the transition to the quark matter during the evolution of matter toward the BH formation; the first order transition, the crossover transition, and the CP sweep, where the BH formation profile goes below, above and through the critical line in asymmetric matter.

The predicted CP locations in lattice MC [26,27,28] and effective models [6] seem to be in the (T, μ_B) region probed in heavy-ion collisions [29,30] or during the prompt black hole formation processes [6] as shown in the right panel of Fig. 4. Recent LQCD-MC predictions by using the reweighting (LR04) [26], Taylor expansion (LT04) [27], and canonical ensemble method (LC11) [28] are consistent with each other, and suggest that the CP is accessible in heavy-ion collisions. It should be noted that some previous studies [31] predicted larger μ_{CP}, and there is also implication that there is no chiral critical point in the small μ region for $N_f = 3$ [32]. By comparison, effective models generally predict the CP in the lower T and larger μ region, and many of them are accessible during the black hole formation. Further studies are necessary to understand the difference between the lattice MC and effective model results.

4. Summary and discussion

We have discussed here two subjects on the QCD phase diagram at finite density. One of them is the chiral and Z_{N_c} deconfinement transition boundaries at finite μ. In the strong coupling lattice QCD with Polyakov loop effects [5], the Z_{N_c} deconfinement boundary defined as the peak of $d\ell/dT$ is found to deviate from the chiral transition boundary at finite μ, and it suggests the existence of the Polyakov loop suppressed high density matter, which may be interpreted as quarkyonic matter [4]. This would be consistent with the lattice QCD Monte Carlo simulation results [7], which suggests that the Z_{N_c} deconfinement transition temperature $T_c(\mathrm{Pol.})$ would be meaningfully higher than the chiral transition temperature $T_c(\chi)$ at $\mu = 0$. The chemical potential effects should be stronger at $T_c(\chi)$ than at $T_c(\mathrm{Pol.})$, then separation at $\mu = 0$ $(T_c(\chi) > T_c(\mathrm{Pol.}))$ would be enhanced at finite μ. This contradicts the results including additional chiral–Polyakov coupling, or the chemical potential dependence of the Polyakov loop potential [10]. In the strong coupling lattice QCD, the additional chiral–Polyakov coupling appears in the higher order terms of the large-dimensional $(1/d)$ expansion, and its effects should be studied.

The possibility of probing the QCD critical point during black hole formation processes is discussed in the second part [6]. We have found that the critical point in isospin asymmetric matter would be accessible in the black hole formation processes, if the CP is in the low T and high μ region as

predicted in chiral effective models. It should be noted that we compare the results of the CP location in chiral effective models and the thermodynamical condition (T, μ_B) calculated with the hadronic EOS. This comparison is relevant, since the thermal trajectory should be the same, even if we use the combined EOS of quark and hadronic matter, as long as the hadronic EOS is reproduced at low T and μ_B in the combined EOS. It is desired to examine the thermodynamical evolution in the combined EOS. Another interesting point is the differences of the CP locations in chiral effective models and in lattice MC simulations. While lattice MC simulations have the sign problem and there is also implications that there is no chiral critical point in the low μ region [32], recent results consistently suggest the CP may exist in the low chemical potential region, $\mu_{CP} \simeq 500$ MeV. It would be necessary to understand these differences in order to pin down the CP location in the phase diagram.

REFERENCES

[1] See for example, G. Odyniec, *Acta Phys. Pol. B* **40**, 1237 (2009).

[2] See for example, N. Abgrall *et al.* [NA61 Collaboration], *PoS* **CPOD2009**, 049 (2009).

[3] P. Demorest *et al.*, *Nature* **467**, 1081 (2010).

[4] L. McLerran, R.D. Pisarski, *Nucl. Phys.* **A796**, 83 (2007).

[5] K. Miura, T.Z. Nakano, A. Ohnishi, N. Kawamoto, `arXiv:1106.1219v1 [hep-lat]`; *PoS* **LATTICE2010**, 202 (2010); T.Z. Nakano, K. Miura, A. Ohnishi, *Phys. Rev.* **D83**, 016014 (2011); *PoS* **LATTICE2010**, 205 (2010).

[6] A. Ohnishi *et al.*, *Phys. Lett.* **B704**, 284 (2011).

[7] Y. Aoki, Z. Fodor, S.D. Katz, K.K. Szabo, *Phys. Lett.* **B643**, 46 (2006).

[8] K. Fukushima, *Phys. Rev.* **D77**, 114028 (2008); L. McLerran, K. Redlich, C. Sasaki, *Nucl. Phys.* **A824**, 86 (2009).

[9] T. Kahara, K. Tuominen, *Phys. Rev.* **D78**, 034015 (2008).

[10] K. Fukushima, *Phys. Lett.* **B695**, 387 (2011); T.K. Herbst, J.M. Pawlowski, B.J. Schaefer, *Phys. Lett.* **B696**, 58 (2011).

[11] K.G. Wilson, *Phys. Rev.* **D10**, 2445 (1974); M. Creutz, *Phys. Rev.* **D21**, 2308 (1980); G. Münster, *Nucl. Phys.* **B180**, 23 (1981).

[12] J. Langelage, G. Munster, O. Philipsen, *J. High Energy Phys.* **0807**, 036 (2008).

[13] N. Kawamoto, J. Smit, *Nucl. Phys.* **B192**, 100 (1981); P.H. Damgaard, N. Kawamoto, K. Shigemoto, *Phys. Rev. Lett.* **53**, 2211 (1984); N. Bilic, F. Karsch, K. Redlich, *Phys. Rev.* **D45**, 3228 (1992).

[14] T.Z. Nakano, K. Miura, A. Ohnishi, *Prog. Theor. Phys.* **123**, 825 (2010); K. Miura, T.Z. Nakano, A. Ohnishi, N. Kawamoto, *Phys. Rev.* **D80**, 074034 (2009); K. Miura, T.Z. Nakano, A. Ohnishi, *Prog. Theor. Phys.* **122**, 1045 (2009).

[15] H. Kluberg-Stern, A. Morel, B. Petersson, *Nucl. Phys.* **B215**, 527 (1983).

[16] K. Fukushima, *Phys. Rev.* **D68**, 045004 (2003).

[17] T. Hatsuda, *Mod. Phys. Lett.* **A2**, 805 (1987); I. Sagert *et al.*, *Phys. Rev. Lett.* **102**, 081101 (2009).

[18] S.J. Smartt, J.J. Eldridge, R.M. Crockett, J.R. Maund, *MNRAS* **395**, 1409 (2009) [arXiv:0809.0403 [astro-ph]]; K.'i. Nomoto *et al.*, *Nucl. Phys.* **A777**, 424 (2006).

[19] K. Sumiyoshi, S. Yamada, H. Suzuki, S. Chiba, *Phys. Rev. Lett.* **97**, 091101 (2006); K. Sumiyoshi *et al.*, *Astrophys. J. Lett.* **690**, 43 (2009); K.'i. Nakazato *et al.*, *Astrophys. J.* **745**, 197 (2012).

[20] C. Ishizuka *et al.*, *J. Phys. G* **35**, 085201 (2008).

[21] Y. Nambu, G. Jona-Lasinio, *Phys. Rev.* **122**, 345 (1961); *Phys. Rev.* **124**, 246 (1961); T. Hatsuda, T. Kunihiro, *Phys. Rep.* **247**, 221 (1994).

[22] S. Roessner, C. Ratti, W. Weise, *Phys. Rev.* **D75**, 034007 (2007); K. Morita, V. Skokov, B. Friman, K. Redlich, *Phys. Rev.* **D84**, 076009 (2011).

[23] K. Kashiwa, H. Kouno, M. Matsuzaki, M. Yahiro, *Phys. Lett.* **B662**, 26 (2008).

[24] V. Skokov *et al.*, *Phys. Rev.* **D82**, 034029 (2010).

[25] A. Ohnishi, D. Jido, T. Sekihara, K. Tsubakihara, *Phys. Rev.* **C80**, 038202 (2009).

[26] Z. Fodor, S.D. Katz, *J. High Energy Phys.* **0404**, 050 (2004).

[27] S. Ejiri *et al.*, *Prog. Theor. Phys. Suppl.* **153**, 118 (2004).

[28] A. Li, A. Alexandru, K.-F. Liu, *Phys. Rev.* **D84**, 071503 (2011).

[29] A. Andronic, P. Braun-Munzinger, J. Stachel, *Nucl. Phys.* **A772**, 167 (2006).

[30] M.A. Stephanov, *Prog. Theor. Phys. Suppl.* **153**, 139 (2004).

[31] Z. Fodor, S.D. Katz, *J. High Energy Phys.* **0203**, 014 (2002); S. Ejiri, *Phys. Rev.* **D78**, 074507 (2008).

[32] P. de Forcrand, O. Philipsen, *J. High Energy Phys.* **0701**, 077 (2007); *J. High Energy Phys.* **0811**, 012 (2008).